Powder Technology 238 (2013) 122–131

Contents lists available at SciVerse ScienceDirect

Powder Technology

journal homepage: www.elsevier.com/locate/powtec

Derivation of parameters for a two compartment population balance model of Wurster fluidised bed granulation

Matthias Börner *, Mirko Peglow, Evangelos Tsotsas

NaWiTec, Thermal Process Engineering, Otto-von-Guericke University Magdeburg, Universitätsplatz 2, 39106 Magdeburg, Germany

ARTICLE INFO

Available online 13 April 2012

Keywords:
Fluidised bed
Internal riser
Wurster granulation
PBM compartment model

ABSTRACT

A common technology for granulation processes is the fluidised bed bottom-spray. This technology can be improved by the use of an internal riser, a so-called Wurster tube. The internal riser has advantages in terms of system stability and enhanced control of particle growth. To mathematically describe the particle growth in such an equipment population balance models (PBM) are applied. These models can be extended by subdivision into a spray compartment and a drying compartment. Important parameters in the compartment models are the compartment size and the particle residence time. In this work, residence time distributions in the riser spray compartment are obtained by a simple gas–particle flow model. The model validity is proven by Particle Image Velocimetry (PIV) and image analysis measurements in a flat test facility. By using an extended PBM it is shown that the particle size distribution (PSD) of the product is not only influenced by the existence of two compartments, but also by the particle size dependent residence time in the spray compartment, which causes additional broadening and skewness. The influence of riser design on particle motion, circulation patterns and product PSD is discussed on the basis of experimental and computational results.

1. Introduction

Fluidised bed technology is frequently applied to the large-scale production of granular materials due to its versatility and potential to conduct granulation or agglomeration at low cost. The resulting coated or aggregated powder particles have added-value with advantages in transportation, solubility, protection or controlled release of active ingredients. In industrial applications different fluidised bed technologies are used (top-spray, bottom-spray, spouted bed etc.) to attain desired granular properties for different products. Especially for coating purposes the fluidised bed bottom spray process offers the most benefits. Large gas and particle velocities nearby the spray prevent agglomeration and enable uniform coating of high quality. An extension of the bottom-spray process can be achieved using an internal riser or a so-called Wurster tube. The internal riser is centrally adjusted above the outlet of a two-component nozzle and particles are forced to move upwards within the tube while being wetted. Accordingly, the circulatory motion of particles and the wetting are more controlled with less variability than in conventional fluidised beds. An additionally installed riser thus changes completely the particle flow pattern of a bottom spray process, leading to a specific and distinct technology for granulation. Fluidised bed equipment with internal riser was firstly introduced by Wurster [1] for the coating of drug particles. Wurster investigated a system, in which an upward moving air stream mixed with atomised coating solution lifts and coats particles in a vertical column.

In recent research the description of particle motion in such fluidised beds attracted significant attention. The knowledge about flow structure, particle residence times and re-circulation behaviour provides the process design to achieve specific product qualities. Such flow investigations of solid motions were conducted by Cronin et al. [2] who derived an analytical description to predict particle residence times in a full circulatory motion. Another interesting approach was presented by Fries et al. [3]. He applied coupled DEM-CFD models to compute the solids flow for extracting spatial information on particle scale.

Observing a batch granulation in a fluidised bed, each particle participates in a re-circulation. After a certain time the particles will pass the spray nozzle. The surrounding domain of nozzle can be defined as so-called spray zone. In this domain particle coating takes place. In the remaining parts of the fluidised bed established coating layers are drying, so this domain is called drying zone. This kind of process space subdivision was first mentioned by Sherony [4] who tried to describe the particle exchange rate and residence times in these characteristic compartments by a stochastical model of surface renewal. These two zones were then considered as perfect mixers for the solid phase [5]. Later a third zone is added [6] to the process subdivision which was a non-active domain with regards to granulation.

In contrast to the consideration of these domains as perfect mixer the re-circulation is significantly influenced by the flow conditions in the bed. That applies most clearly to the spray zone. Different particle properties and the dominant gas jet lead to a non-uniformity in particle transport and thus for unsteady coating and particle growth behaviour.

* Corresponding author.
E-mail address: Matthias.Boerner@ovgu.de (M. Börner).
URL: http://www.nawitec.org (M. Börner).

0032-5910/$ – see front matter © 2012 Elsevier B.V. All rights reserved.
doi:10.1016/j.powtec.2012.04.014

As solution to the described irregular coating the particle growth can be considered in dependence of different particle properties and flow conditions in bed. The particle growth is hereby described by a population balance model (PBM) with reference to Hoffmann et al. [7]. The model considers two spatial compartments, the spray compartment and the drying compartment. In contrast to other approaches [8,9] the growth rate term used in the model is independent of the particle size and proportional to the particle surface [10]. So the dependence of particle properties and specifically of their sizes on the particle growth is given by the particle flow properties. These flow properties and the variability of flow conditions can be described best by the particle residence time and its distribution. The residence time distributions are obtained by a mathematical gas–particle flow model. The model can predict the fluid flow conditions and the particle motions within the riser i.e. in the spray zone. The validity of the model was verified by measurements of Particle Image Velocimetry (PIV) to determine particle velocities, and image analysis for estimating solids volume fraction. The fluidised bed used is a flat construction, which has been applied for hydrodynamic investigations. In such fluidised beds a two-dimensional flow characteristic can be realised. This experimental approach was applied by several authors for instance to describe segregation effects [11,12], for the validation of the results of CFD and DEM simulations [13–16] or for investigation of bubble behaviour and their characteristics in fluidised beds [17–20].

The aim of the performed investigations is to show the size-dependent compartment exchange for the spray zone of a Wurster fluidised bed granulation. In the spray compartment exists the most significant influences caused by the flow properties, being the reason for their systematic consideration on the particle growth behaviour.

2. Theory

2.1. Population balance model (PBM)

The mathematical description of a batch fluidised bed granulation is implemented by applying a one-dimensional two compartment population balance model (PBM) described by Hoffmann et al. [7] in which particle size is the only internal coordinate. In this relatively simple PBM approach particle agglomeration, breakage, attrition or nucleation is neglected. In the PBM two compartments are considered. One compartment is the spray zone α, where particle wetting takes place, and the second compartment is the drying zone $(1-\alpha)$, characterised by solidification of previously applied coating layers. This compartment separation requires knowledge about associated particle residence times τ, which express the ratio of compartment hold-up m to the compartment exchange mass flow rate M of particles. For the spray compartment α and its contained number distribution function of particles n_α the population balance equation results in:

$$\frac{\partial n_\alpha}{\partial t} = -\frac{\partial (G n_\alpha)}{\partial d_p} - \frac{n_\alpha}{\tau_\alpha} + \frac{n_{1-\alpha}}{\tau_{1-\alpha}} \tag{1}$$

and accordingly for the drying compartment $1-\alpha$

$$\frac{\partial n_{1-\alpha}}{\partial t} = \frac{n_\alpha}{\tau_\alpha} + \frac{n_{1-\alpha}}{\tau_{1-\alpha}}. \tag{2}$$

The change within the number distribution function is dependent on process conditions which are reflected by the particle growth rate G.

$$G = \frac{dm_p}{dt}. \tag{3}$$

The growth kinetics expressed by G, the change of particle mass m_p per time unit t, can be generalised in such a way that the droplet deposition on the particle surface is proportional related to any moment μ_i of the particle size distribution. Among these can be the moment of particle number $(i=0)$, particle length $(i=1)$, particle surface area $(i=2)$ or particle volume $i=3$. Therefore, the general approach for the growth rate is:

$$G_i = \frac{2M_l d_p^{i-2}}{\rho_p \pi \mu_i}. \tag{4}$$

The growth rate can further be determined by linear combination of different growth kinetics

$$\overline{G} = \sum_{i=0}^{I} \lambda_i G_i \tag{5}$$

with

$$\sum_{i=0}^{I} \lambda_i = 1. \tag{6}$$

In the later calculation of particle growth kinetics the surface area proportional moment μ_2 is considered.

$$G_2 = \frac{2M_l}{\rho_p \pi \mu_i} = \frac{2M_l}{\rho_p A_{ges}}. \tag{7}$$

That accounts for a particle size independent growth term [10]. For all other moments the growth rate is particle size dependent and proportional to droplet deposition. The partial PBM equations are transformed in ordinary differential equations of the following discretised scheme:

$$\frac{dN_j}{dt} = \frac{\overline{G}_j N_j - \overline{G}_{j-1} N_{j-1}}{\Delta d_p}. \tag{8}$$

By applying the Flux-limiter method the PBM was solved.

2.2. Residence time model

The PBM needs explicit information about the particle residence time in the two considered compartments. The residence time is dependent on the system configuration as well as on adjustable process parameters and particle properties. For the fluidised bed bottom spray process with an internal riser a gas–particle flow model is applied in order to obtain the required particle residence times. The developed flow model is a simple approach that approximates the steady gas flow conditions in the spray zone and the particle motions induced by the fluid flow. Such simplified approach can be applied since the flow conditions inside the riser are quite uniform developed. The flow field consists of a constant fluidisation gas flow with gas velocity u_{fl} originating from the bottom distributor and a gas jet created by the spray nozzle. The two gas flows are superimposed in the same direction, so that the gas velocity flow field u can be described by:

$$u(s,r) = u_{jet} + u_{fl}. \tag{9}$$

The gas jet and its gas velocity u_{jet} can be analytically described by a turbulent free jet model in accordance with Truckenbrodt [21]. The fluid mechanics of the free jet marks a boundary layer flow problem with a friction afflicted interlayer between two commutated fluid flows. The gas velocity profile can be sufficiently described by an error function,

$$u_{jet} = e^{-C\eta^2} u_{max} \tag{10}$$

where u_{max} is the maximum jet velocity dependent on the jet path length s, $C = \ln 2$ is a constant, and $\eta = r/r_{jet}$ is the reduced radial coordinate; r_{jet} is thereby the lateral border line of the free jet lying on an expansion angle ϕ of 9°, see Fig. 1. A particularity of a free jet is the aspiration of surrounding gas in accordance with an increasing mass flow rate along its flow path. However, when the jet approaches the riser at a path length of $s = h_r$, this particular condition will not be valid anymore. The riser inhibits the aspiration of gas and the gas mass flow rate becomes constant from this location on. Consequently, at isothermal conditions the integral of the gas velocity across the total riser width also becomes constant:

$$\int_0^{2r_r} u(r)dr_r = const. \tag{11}$$

Within the riser the jet flow will turn over to a turbulent tube flow. Since the flow profile is known at the location h_r, a damping function is applied in order to switch to a flattened turbulent velocity profile. To achieve the flattening of the velocity profile the constant C in Eq. (10) is linearly adapted:

$$C_2 = \frac{\beta - C}{s_{in}}(s - h_r) + C. \tag{12}$$

The adaption takes place along a characteristic inflow path, u_{max} and η being kept at their values for the location $s = h_r$. To reproduce a fully developed turbulent velocity profile [22], β was determined with 0.04. After the inflow path of approximately $s_{in} = 2r_r$, derived from measured particle velocity profiles, the damping coefficient C_2 is kept at $C_2 = \beta$. During the described transition, Eq. (11) of mass conservation has to be guaranteed. For this purpose a normalisation parameter C_3 is introduced and determined to fulfil the condition

$$\int_0^{2r_r} u(h_r, r)dr_r = \int_0^{2r_r} u(s > h_r, C_3, r)dr_r. \tag{13}$$

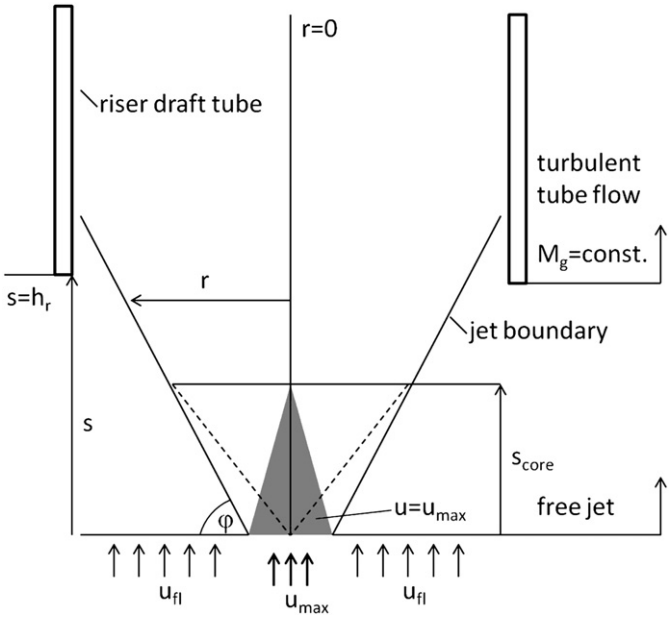

Fig. 1. Schematic illustration of flow field.

In total the turbulent gas velocity within the riser is obtained to

$$u_r = e^{-C_2(s)\eta^2(h_r)}u_{max}C_3 + u_{fl}. \tag{14}$$

The particles that move in the gas flow field underlie Newton's second law of motion. For gas–solid systems with large density differences the momentum balance can be simplified to

$$m_p \frac{dv}{dt} = F_D - F_G, \tag{15}$$

where F_G is the weight force and F_D is the drag force, both acting on each particle. The drag force is expressed by:

$$F_D = 0.5 c_{D,\alpha}\rho_g A_{proj}(u - v)^2 \tag{16}$$

where A_{proj} is the projection area of a particle and $c_{D,\alpha}$ the drag coefficient in the spray compartment. The drag coefficient is first obtained to c_D according to Clift and Gauvin [23]. The Clift drag model has good performance for single particles and particles moving in a spouted gas flow [24]. Then, the drag coefficient c_D is corrected with the particle volume fraction $\epsilon_{p,\alpha}$ to obtain

$$c_{D,\alpha} = c_D\left(1 - \epsilon_{p,\alpha}\right)^p. \tag{17}$$

In this way, an increased drag force at larger particle volume fractions can be considered [25]. According to Wen and Yu [26] the exponent p in Eq. (17) takes into account the present particle Reynolds numbers. For the acquisition of particle residence times in both compartments the geometric dimensions of either zone have to be defined. In the Wurster fluidised bed the spray zone α can be considered to consist of the domain inside the riser and the gap between spray nozzle and riser, as depicted in Fig. 2. By this assumption, spraying on particles and mixing with droplets only take place in this limited spatial domain. In the fountain zone above the riser and in the bubbling bed drying of already deposited coating layers occurs, defined as the drying compartment $1 - \alpha$.

For validation of the gas–particle flow model and derivation of necessary model parameters experimental investigations were conducted. The experimental configuration used for this purpose is described in detail in Section 3. A comparison between model predicted and measured particle velocities in the middle plane of the spray compartment is shown in Fig. 3. Therefore it can be concluded that the model can predict the particle flow sufficiently well.

The particle residence time in the spray compartment is derived from particle velocity to

$$\tau_\alpha = \int_0^{l_\alpha} \frac{ds}{v}. \tag{18}$$

Thereby the travel path is the length of the spray compartment l_α, which is the sum of riser mounting height h_r and riser length l_r. However, the inflow and the travel paths can be a function of radial position. For the case of particles entering the jet in higher locations the particle entrance can have a displacement in radius r. Particles entering in higher location mostly pass along the outer border of the riser and become less accelerated compared to particles entering at $r = 0$. This is based on a smaller relative velocity between gas and particles. As a simplification the differentiation of the radial entrance position is not accounted for in this approach considering a spatial dependent particle residence times within the spray zone. In this regard for each particle size a corresponding residence time value is determined for each gas flow condition using the entrance position $r = 0$. The residence time distribution results in this context by considering different particle diameters.

The initial particle entrance velocity into the jet is set to $v_{s=0}=0$, since particle motions in the bottom of the bed are mainly horizontally directed with negligible vertical velocity component.

In the two compartment separation the residence time in the drying compartment $1-\alpha$ can be determined as function of the spray compartment based on the fact that the inflow into the drying compartment is identical with the outflow of the spray compartment.

$$\tau_{1-\alpha}=\tau_{\alpha}\left(\frac{1}{\alpha}-1\right) \tag{19}$$

In Eq. (19), α is the fraction of total particle mass contained in the spray compartment. This can be calculated from the measured mean particle volume fraction $_{p,\alpha}$ and the spray compartment volume V_{α}.

$$\alpha=\frac{V_{\alpha}\rho_{p}\epsilon_{p,\alpha}}{m_{bed}}. \tag{20}$$

With regard to a particle number basis, Eq. (20) results in:

$$\alpha=\frac{\sum_{i=0}^{N} n_{\alpha}\Delta d_{p,i}d_{p,i}^{3}}{\sum_{i=0}^{N}(n_{\alpha}+n_{1-\alpha})\Delta d_{p,i}d_{p,i}^{3}} \tag{21}$$

where $\Delta d_{p,i}$ is the width of the particle size class and $d_{p,i}$ the class mid value. The fractional hold-up of the drying department is simply $1-\alpha$.

3. Experimental methods

The best ways to evaluate or validate model parameters and to investigate particle dynamics are experimental trials. In the trials performed a flat, transparent fluidised bed with rectangular cross section was used. The dimensions of the fluidised bed were $300\times 20\times 1000\ mm^3$ (width × depth × height) and its schematic illustration is depicted in Fig. 4. Particle fluidisation was realised on the outer sides of the bottom of the bed by two distributor plates. In between a nozzle segment was inserted. Above the distributor plate two draft plates were adjusted constituting the internal riser. In various experiments these draft plates can be changed in position (height of gap) and design (length, width, shape).

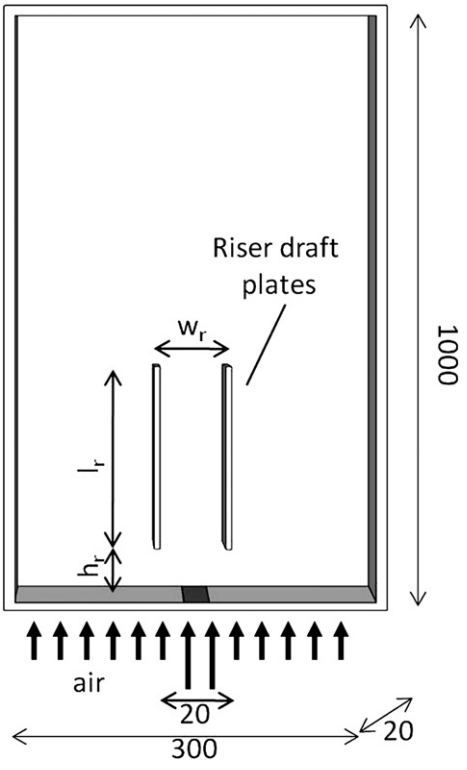

Fig. 2. Compartment separation in the Wurster fluidised bed granulator; α: spray compartment and $(1-\alpha)$: drying compartment.

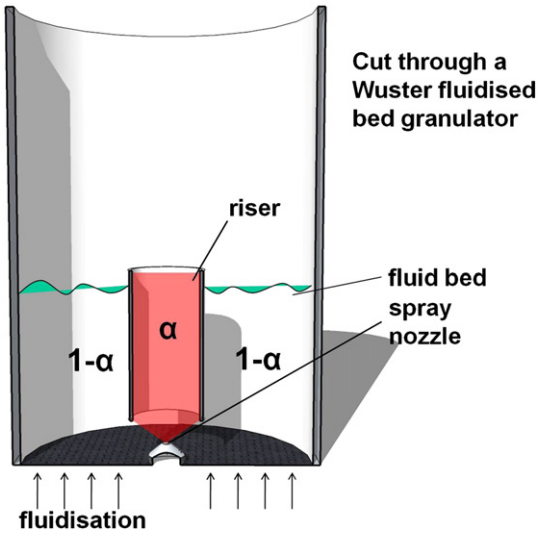

Fig. 3. Validation of gas–particle flow model by comparison of PIV measurements with model predictions for the configuration with $w_r=30$ mm riser width and $l_{\alpha}=h_r+l_r=206$ mm spray compartment length; particle velocities refer to the central axis of the riser/spray compartment.

The transparent walls of the fluidised bed permit the observation and analysis of particle dynamics and their motions, which were recorded by a digital camera. From the recorded images the particle velocity was determined applying Particle Image Velocimetry (PIV) for densely seeded flows [27–29]. Particle shifts between two recorded images are determined by the application of a cross correlation without a direct particle tracking. The time delay between two consecutive images is chosen to be at a frequency of 1 kHz, and the next two images are recorded after 0.1 s. The entire measurement time comprises 100 s in total for each trial. The spatial resolution of the velocity determination is set by a single interrogation area size of 8-by-8 mm with 50% overlap with adjacent interrogation areas to resolve a detailed particle circulation pattern.

As a second measurement technique particle volume fractions are estimated from the images by means of the digital image analysis (DIA) algorithm of van Buijtenen et al. [30]. Hereby, values of the two-dimensional particle volume fraction ϵ_p^{2D} in the interrogation areas are transformed to the volumetric particle concentration ϵ_p. Both methods of image analysis provide information about solid motion and dispersion behaviour within the multiphase flow. Measured data will be later compared with model predictions and are used to describe the particle flow characteristic in the internal riser. Furthermore, the measurements provide data needed in the proposed model, namely the particle volume fraction in the spray compartment. Parameters of the experimental investigations are listed in Table 1.

4. Results

4.1. Particle flow characteristics

One of the objectives in this work was to investigate how the particle flow behaviour in the bed changes for different riser configurations. Especially the sizing of the riser can have significant influence on the occurring flow structures and thus on the spray compartment shape. In industrial granulation processes the minimal possible input

of gas for fluidisation as well as optimal wetting in the spray compartment and with an efficient drying and solidification of the coating in the outer bed, is of particular interest. As little gas as possible shall be bypassing the bed in the form of bubbles to keep heat and mass transfer high, preserving a good solid mixing as well as a continuous circulation of particles. This would be in favour of fast drying with narrow particle residence time distributions within both compartments and leading to more uniform particle coatings.

In the riser three phases – liquid droplets, solids and gas – are present, and collisions between droplets and particles occur. High relative velocity between gas and particles should favour the coating process, preventing inter-particle collisions that would lead to undesired agglomeration. Inside the riser, particles are indeed undisturbed and continuously accelerated until its end. The flow conditions in the riser are comparable with circulating fluidised beds in turbulent or transport regime. Meanwhile the transported particles are mixed with droplets. Conventionally particles reach a smaller velocity than atomised droplets, because of the solids' greater size and density. So collisions between droplets and particles can occur along the entire length of the riser. The velocity difference during such collisions decides whether a droplet will deposit for coating or rebound. This is essential for the rate of granulation or for a potential discharge of unused droplets.

In this regard the riser length l_r is indeed one of the most relevant configuration parameters. The riser length determines the travel path of particles, duration of acting drag force and the size of the domain for particle surface wetting. Generally, the riser length has to exceed the height of the outer fluidised bed of particles. That guarantees clear boundaries of an unaffected wetting zone. Further, the fall back of particles from the bed into the riser shall be avoided to ensure a stable and straight upwards-directed particle flow in the riser/spray compartment.

The height h_r of placement of the riser above the distributor plate decides about both, the aspiration of particles into the nozzle jet and the stability of particle flow inside the riser. Basically it can be said that the larger the gap between riser and bottom gas distributor is, the more particles can enter the upward jet. By manipulating the height h_r the particle mass flow rate and the particle volume fraction in the spray compartment can be adjusted. This particle volume fraction is further dependent on the fluidisation and nozzle mass flow rates, see Table 2. The distribution of particles in the riser and their corresponding velocities are shown in Fig. 5. However, if h_r exceeds a certain level, dependent on the particle size and material properties, the particle aspiration into the jet does not proceed stably anymore. An intermittent particle inflow is then observed and causes inhomogeneous particle concentrations, similarly to a spout fluidised bed.

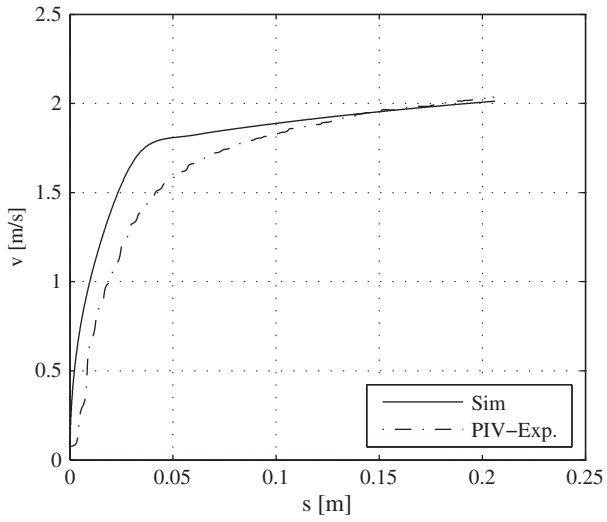

Fig. 4. Experimental setup of the flat, transparent fluidised bed; dimensions in mm.

Table 1
Product properties and parameters in the experimental investigations.

Product	γ-alumina
d_p	1.8 mm
ρ_p	1040 kg m^{-3}
u_{mf}	0.56 m s^{-1}
m_{bed}	0.515 kg
h_{fb}	0.15 m
h_r	0.026 m
l_r	0.115, 0.18 m
w_r	0.03, 0.04 m
M_{jet}	15, 20 kg h^{-1}
u_{fl}	0.7, 0.84, 1.12 m s^{-1}

Beyond this gas velocity level the mass flow of solids through the riser almost keeps constant with a mean solids volume fraction in the riser around $\epsilon_p = 0.15$. In rough estimation the transition to an intermittent flow occurs at a height h_r of approximately 20 times the particle diameter. This aspect was investigated by using, in addition to the 1.8 mm γ-alumina spheres of Table 1, also smaller particles of this kind, with a diameter of 1 mm. However, there are several impacts on this transition point, such as fluidisation velocity, type of distributor etc., which makes general predictions difficult.

Another essential design parameter is the diameter or width w_r of the riser. This parameter mainly influences the gas flow conditions inside the riser, and thus the drag on the particles. The smaller the diameter chosen the higher are the gas velocity and accordingly also particle velocities that can be achieved. On the one hand, a shorter particle residence time in the spray compartment is present, on the other hand particles reach larger fountain heights. The differences for the widths $w_r = 30$ mm and $w_r = 40$ mm are illustrated in streamlines for different flow conditions, see Fig. 6. The streamlines were obtained from PIV measurements by averaging over the entire duration of the measurements of about 100 s.

In the streamlines the main circulatory motions of particles can be observed. Derived from these PIV measurements the mean particle velocity in the spray compartment α and hence the particle residence time τ_α can be determined. By Eq. (19) the residence time in the drying compartment can be computed and the sum of the two characteristic times gives the mean re-circulation time τ_{re} for a particle's full circulatory motion. Residence times gained from measured values for the test material γ-alumina with diameter 1.8 mm are listed in Table 3. Moreover, the experimental values are compared with residence times computed by the model of Section 2.2. This comparison shows a good agreement. It should be noticed that both, the experimental acquisition methods and the model consider only particles that ascend straight upwards in the centre of the spray compartment.

Depending on equipment and process design, dead zones within the bed can exist. Such dead zones can be detected by the applied measurement techniques. Three different locations can be distinguished, which are schematically illustrated in Fig. 7. The dead zones of types 1 and 2 are characterised by static particles that hardly participate in the re-circulation process. This causes irregular circulatory motions in the bed and can further evoke deviations in residence time. Dead zones of type 2 are usually avoided by reducing the bed diameter at the bottom and expanding it at larger bed heights. Zones of type 1 can be impeded

Table 2
Measured mean particle volume fractions and mean particle velocities inside the riser, dependent on the gas flow conditions; $w_r = 40$ mm.

$f = u_{fl}/u_{mf}$	1.25	1.25	2.0	2.0
M_{jet} [kg/h]	15	20	15	20
$\overline{\epsilon_p}$ [–]	0.153	0.107	0.125	0.099
v [m/s]	1.32	1.71	1.25	1.65

by a higher fluidisation or with alternative riser shapes which simply eliminate the outline of the zone geometrically. Both types of zones can be observed in the streamline plots. Here, the streamlines get lost or suddenly end. Within dead zones of type 3 no particles are contained. The shape of the zone depends on the width of the riser w_r, the entrance height of the riser h_r and the spray conus of the nozzle. This zone occurs since particles are only entrained in the gas jet at high gas velocity. Regions of small gas velocities will not be entered by particles.

4.2. Particle size dependent residence times

As a second objective of this work, the impact of different spray compartment configurations on the residence time distribution and particle growth behaviour shall now be exposed. In this context a distributed particle size is assumed. By different particle sizes the particle residence time in the spray compartment differs, whereby larger particles stay longer compared to smaller particles. This residence time bandwidth affects the particle growth rate since larger particles have more time to get in contact with droplets of binder, and it shall be proven how much faster the larger particles can grow. For the interval of 0.1 to 1.5 mm particle diameter the particle residence times in the spray compartment are determined by the gas–particle flow model. Discrete computed values are represented by a continuous relation applying a polynomial function of third order. The results for three different riser widths are depicted in Fig. 8. Here, the gas flow of jet is adjusted to 5 kg/h, which is deliverably quite low for the set of configurations. In this way a broad residence time distribution is obtained to better show possible influences and to demonstrate the consequences on the particle growth afterwards. By the use of an enlarged riser width the spray compartment size is increased. This reduces the mean gas velocity and, consequently, also the bed height and the acceleration of particles. Under such conditions broader particle residence time distributions can appear. A further decisive influence on the particle residence time is exerted by the nozzle mass flow rate. This dependency is illustrated in Fig. 9. The throughput of the nozzle substantially determines the gas velocities in the riser and therewith the particle acceleration. The higher the mass flow rate, the narrower is the residence time distribution that can be achieved. Concluding, the mentioned variables, comprising particle size, spray compartment size and nozzle mass flow rate, strongly influence the particle residence time behaviour in the spray compartment leading to a characteristic distribution with further impact on the growth behaviour.

The residence time in the drying compartment $\tau_{1-\alpha}$ is on the contrary, not dependent on particle size. Particle size controlled settling in the bubbling bed can be neglected and the fall back from the particle fountain above the riser as well as the re-entry into the spray compartment can be seen as a size independent process. However, it should be noted that the time constant of particle settling is affected by the intensity of fluidisation. Consequently, an average value is sufficient for $\tau_{1-\alpha}$, and it can be calculated by applying Eq. (19) with τ_α for the volume-to-surface mean, d_{32}, of the particle size distribution:

$$\tau_{1-\alpha} = \tau_\alpha(d_{32})\left(\frac{1}{\alpha} - 1\right). \tag{22}$$

4.3. PBM results

The obtained residence time distributions of τ_α are implemented into the PBM of Eqs. (1) and (2) as continuous functions. Accordingly, for every particle size class of number density distribution the corresponding residence time can be determined. To emphasise the attained model

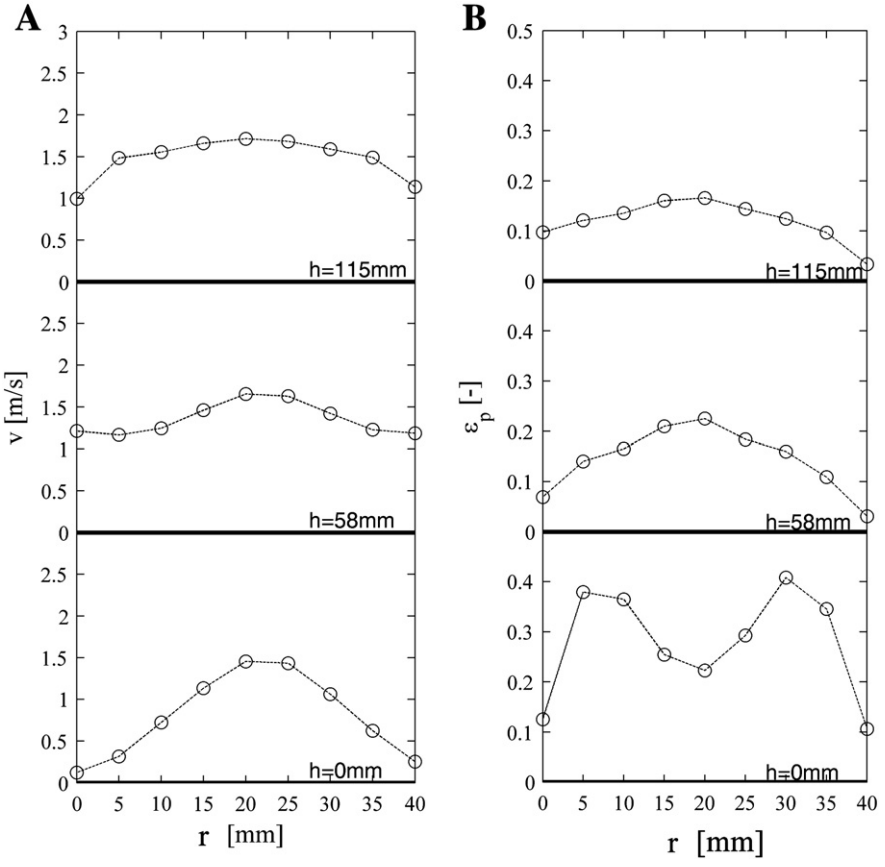

Fig. 5. (A) Measured particle velocity profiles at different heights inside the riser for $w_r = 40$ mm and (B) the corresponding measured distributions of volumetric particle concentration.

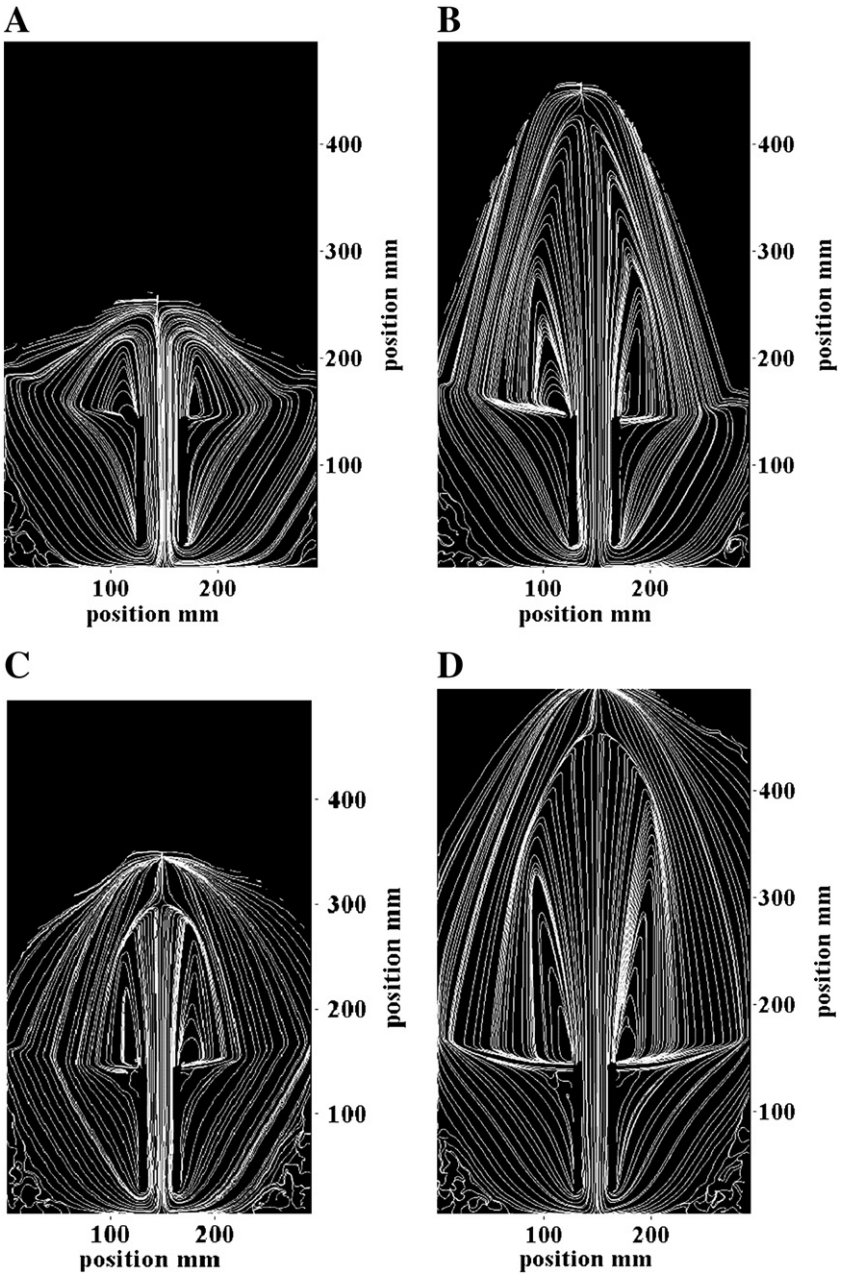

Fig. 6. Measured particle streamlines for (A) $w_r = 40$ mm and $M_{jet} = 15$ kg/h, (B) $w_r = 40$ mm and $\dot{M}_{jet} = 20$ kg/h, (C) $w_r = 30$ mm and $\dot{M}_{jet} = 15$ kg/h, (D) $w_r = 30$ mm and $\dot{M}_{jet} = 20$ kg/h; in all cases $f = 1.25$.

enhancement of a size distributed residence time in the spray compartment and a particle size dependent compartment exchange a comparison with the previous model assumption of a constant residence time is shown in Fig. 10. Here, the volume density function q_3 is computed for a certain process time, starting with an initial particle size distribution in the bed. The constant residence time presented is determined by $\tau_\alpha = 0.2$ s. This residence time corresponds to the mean particle size of the initial size distribution. The final density distributions received after 250 min of process time are compared for the system configuration with a riser width of $w_r = 30$ mm. The general simulation settings are a batch mass of 4 kg and a liquid spray rate of 6 kg/h in respect to common granulation experiments. In Fig. 10 it can be seen that for the constant residence time the initial density distribution is getting broader and shifts to larger particle sizes. However the distribution is still conserving its symmetrical shape. By considering the particle size dependency of the residence time, the effect that larger particles grow faster compared to smaller ones within the spray compartment becomes obvious. The particle size distribution widens faster and attains a higher variance. Additionally some asymmetry towards larger particle diameters is observed. The shape of the distribution conforms better to experimental data of batch granulation processes reported by Hoffmann et al. [7].

Table 3
Particle residence times in the spray compartment α (measured and computed), in the drying compartment $1-\alpha$ (obtained from measurements) and re-circulation times for $w_r = 40$ mm, $l_r = 115$ mm and $f = u/u_{mf}$.

$f = u_{fl}/u_{mf}$	1.25	1.25	1.5	1.5
$\dot{M}_{jet}$ [kg/h]	15	20	15	20
τ_α [s]	0.09	0.07	0.09	0.07
$\tau_{1-\alpha}$ [s]	3.38	4.04	3.04	3.61
τ_{re} [s]	3.47	4.11	3.13	3.70
τ_α model [s]	0.0933	0.0686	0.0916	0.0688

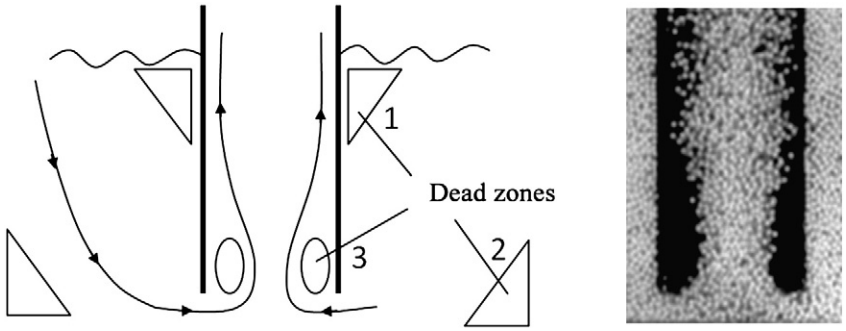

Fig. 7. Dead zones within Wurster fluidised bed equipment; schematical illustration and evidence in image recordings of death zone type 3.

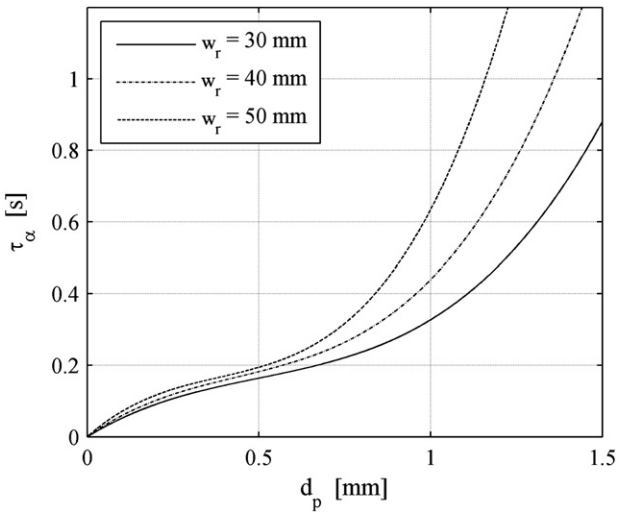

Fig. 8. Dependency of the particle residence time distribution in the spray compartment on riser width; nozzle mass flow rate $\dot{M}_{jet} = 5$ kg/h, $u_{fl} = 0.7$ m/s, riser length $l_r = 180$ mm.

Further, the impact of the riser design on the resulting particle size distribution is of explicit interest. Riser design determines the spray compartment size as well as the flow conditions in this compartment. For the case that all other settings are kept constant and only the riser width is changed, the particle growth is simulated and illustrated in Fig. 11. By using a wider riser construction, a broader particle size distribution with significant tailing to larger particle sizes is obtained. The usually desired narrow size distribution, typical for the fluidised bed with internal riser, cannot be achieved if riser geometry and gas flow are chosen improperly. In general, a narrow riser diameter and large gas velocities in the spray compartment will decrease the difference in residence time between small and large particles and, thus, facilitate a more uniform particle growth.

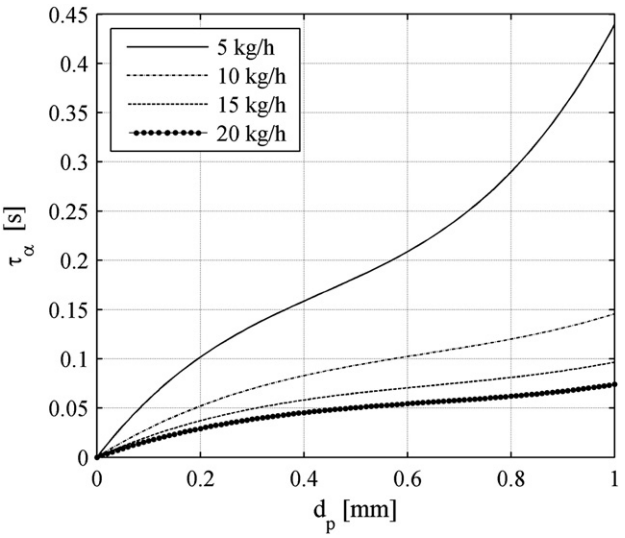

Fig. 9. Dependency of the particle residence time distribution in the spray compartment on nozzle gas mass flow rate; riser width $w_r = 40$ mm, $u_{fl} = 0.7$ m/s, riser length $l_r = 180$ mm.

5. Conclusions

The particle flow and growth behaviour in a fluidised bed with an internal riser have been investigated by applying image measurement techniques, a gas–particle flow model inside the riser, and a one-dimensional two compartment population balance model (PBM). The gas–particle flow model considers the acceleration of particles in a turbulent free jet which turns to turbulent tube flow when approaching the riser draft tube. Acquisition of the necessary model parameters and model validation were conducted by the experimental methods. The results achieved by the flow model were implemented into the PBM to investigate the particle growth behaviour under consideration of a particle size dependent residence time in the spray compartment. Furthermore, the influence of riser design and gas flow conditions on the granulation process was discussed.

From the results it can be concluded that the improved residence time model for the spray compartment based on the consideration of particle dynamics may predict more realistic size distributions compared to a compartment model with constant residence times neglecting a particle size dependent compartment exchange. A further conclusion is that the riser design has significant influence on the flow and growth behaviour. For wider riser constructions the particle growth is less uniform and the resulting distribution will be much broader. To achieve a narrow distribution within such a system, the riser has to be designed with smaller diameter. This leads to more stable flow conditions in the riser tube with less difference in residence time between smaller and larger particles.

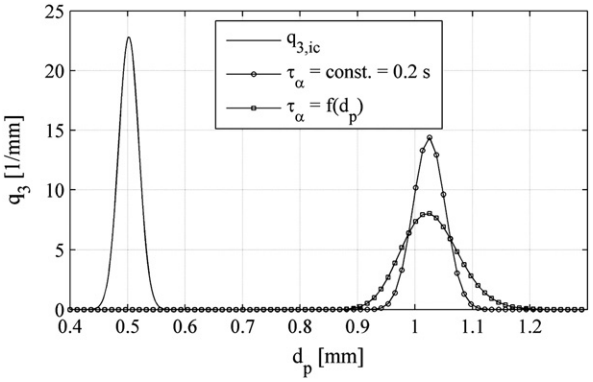

Fig. 10. Comparison of particle size distributions computed either with a constant or with a particle size dependent residence time in the spray compartment; riser width $w_r = 30$ mm, riser length $l_r = 180$ mm, nozzle mass flow rate $\dot{M}_{jet} = 5$ kg/h, $u_{fl} = 0.7$ m/s.

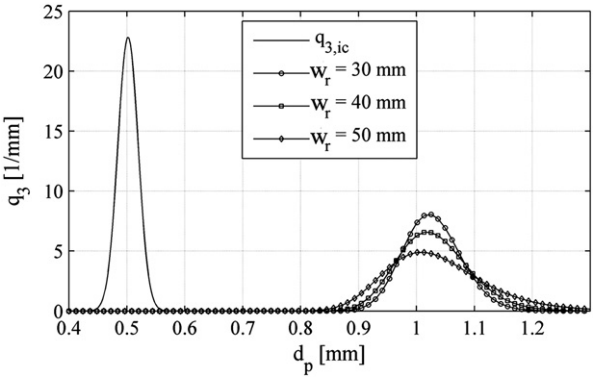

Fig. 11. Particle size distributions for a Wurster granulation process, computed for three different riser widths of 30 mm, 40 mm and 50 mm; riser length $l_r = 180$ mm, nozzle mass flow rate $\dot{M}_{jet} = 5$ kg/h, $u_{fl} = 0.7$ m/s.

Notation

α	mass fraction of solids in spray comp.	[–]
$1-\alpha$	mass fraction of solids in drying comp.	[–]
β	inflow coefficient	[–]
ϵ_p	solid volume fraction	[–]
$\epsilon_{p,\alpha}$	solid volume fraction in spray comp.	[–]
η	non-dimensional jet radius	[–]
λ_i	linear coefficient	[–]
μ_i	moment	[m^i]
ρ_p	particle density	[kg m^{-3}]
ρ_g	gas density	[kg m^{-3}]
τ_α	residence time in spray comp.	[s]
$\tau_{1-\alpha}$	residence time in drying comp.	[s]
τ_{re}	recirculation time	[s]
A_{ges}	total particle surface area	[m^2]
A_{proj}	projection area	[m^2]
$C_{1,2,3}$	constant	[–]
c_D	drag coefficient	[–]
$c_{D,\alpha}$	drag coefficient in spray comp.	[–]
d_p	particle diameter	[m]
d_32	volume-to-surface mean	[m]
f	fluidisation number, u/u_{mf}	[–]
F_D	drag force	[N]
F_G	weight force	[N]
G	growth rate	[m s^{-1}]
h_{fb}	fixed bed height	[m]
h_r	riser entrance height	[m]
i, j	index	[–]
l_r	riser length	[m]
N	number	[–]
n	number distr. function in spray comp.	[m^3]
$n_{1-\alpha}$	number distr. function in drying comp.	[m^3]
M	mass flow rate	[kgs^{-1}]
M_l	mass flow rate of liquid binder	[kg s^{-1}]
M_{jet}	gas mass flow rate through nozzle	[kg s^{-1}]
m_{bed}	total bed mass	[kg]
m_p	particle mass	[kg]
q_3	volume density function	[m^{-1}]
$q_{3,ic}$	q_3 at initial condition	[m^{-1}]
p	Wen & Yu exponent	[–]
r	radius	[m]
r_{jet}	jet radius	[m]
r_r	radius of riser	[m]
s	path length	[m]
t	time	[s]
u	gas velocity	[m s^{-1}]
u_{fl}	fluidisation velocity	[m s^{-1}]
u_{jet}	jet velocity	[m s^{-1}]
u_{max}	max gas velocity in free jet	[m s^{-1}]
u_{mf}	minimum fluidisation velocity	[m s^{-1}]
V_α	spray comp. volume	[m^3]
v	particle velocity	[m s^{-1}]
w_r	riser width	[m]

Acknowledgement

The authors gratefully acknowledge the funding of this work by the German Federal Ministry of Science and Education (BMBF) as part of the InnoProfile project NaWiTec.

References

[1] D.E. Wurster, Air-suspension technique of coating drug particles. A preliminary report, Journal of the American Pharmaceutical Association 48 (1959) 451–454.
[2] K. Cronin, M. Çatak, D. Tellez-Medina, V. Cregan, S. O'Brien, Modelling of particle motion in an internal re-circulatory fluidized bed: pharmaceutical granulation and processing, Chemical Engineering Journal 164 (2010) 393–402.
[3] L. Fries, M. Dosta, S. Antonyuk, S. Heinrich, S. Palzer, Moisture distribution in fluidized beds with liquid injection, Chemical Engineering and Technology 34 (2011) 1076–1084.
[4] D.F. Sherony, A model of surface renewal with application to fluid bed coating of particles, Chemical Engineering Science (1981) 845–848.
[5] P. Wnukowski, The coating of particles in a fluidized bed (residence time distribution in a system of two coupled perfect mixers), Chemical Engineering Science (1989) 493–505.
[6] S. Maronga, P. Wnukowski, Modelling of the three-domain fluidized bed particulate coating process, Chemical Engineering Science 52 (1997) 2915–2925.
[7] T. Hoffmann, M. Peglow, E. Tsotsas, Prozessdynamik der wirbelschichtgranulierung: process dynamics of the fluidized bed granulation, Chemie Ingenieur Technik 83 (2011) 658–664.
[8] L.X. Liu, J.D. Litster, Coating mass distribution from a spouted bed seed coater: experimental and modelling studies, Powder Technology 74 (1993) 259–270.
[9] K. Sudsakorn, R. Turton, Nonuniformity of particle coating on a size distribution of particles in a fluidized bed coater, Powder Technology 110 (2000) 37–43.
[10] S. Heinrich, M. Peglow, M. Ihlow, M. Henneberg, L. Mörl, Analysis of the start-up process in continuous fluidized bed spray granulation by population balance modelling, Chemical Engineering Science 57 (2002) 4369–4390.
[11] M.J.V. Goldschmidt, R. Beetstra, J.A.M. Kuipers, Hydrodynamic modelling of dense gas-fluidised beds: comparison and validation of 3d discrete particle and continuum models, Powder Technology 142 (2004) 23–47.
[12] G. van Bokkers, M. van Sint Annaland, J.A.M. Kuipers, Mixing and segregation in a bidisperse gas–solid fluidised bed: a numerical and experimental study, Powder Technology (2004) 176–186.
[13] F. Taghipour, N. Ellis, C. Wong, Experimental and computational study of gas–solid fluidized bed hydrodynamics, Chemical Engineering Science (2005) 6857–6867.
[14] J. Link, L. Cuypers, N. Deen, J.A.M. Kuipers, Flow regimes in a spout-fluid bed: a combined experimental and simulation study, Chemical Engineering Science (2005) 3425–3442.
[15] F. Hernández-Jiménez, S. Sánchez-Delgado, A. Gómez-García, A. Acosta-Iborra, Comparison between two-fluid model simulations and particle image analysis & velocimetry (piv) results for a two-dimensional gas–solid fluidized bed, Chemical Engineering Science 66 (2011) 3753–3772.
[16] M.S. van Buijtenen, M. Börner, N.G. Deen, S. Heinrich, S. Antonyuk, J.A.M. Kuipers, An experimental study of the effect of collision properties on spout fluidized bed dynamics, Powder Technology 206 (2011) 139–148.
[17] L. Shen, F. Johnsson, B. Leckner, Digital image analysis of hydrodynamics two-dimensional bubbling fluidized beds, Chemical Engineering Science 59 (2004) 2607–2617.
[18] J. Laverman, I. Roghair, M. van Sint Annaland, J.A.M. Kuipers, Investigation into the hydrodynamics of gas–solid fluidized beds using particle image velocimetry coupled with digital image analysis, The Canadian Journal of Chemical Engineering 86 (2008) 523–535.
[19] A. Busciglio, G. Vella, G. Micale, L. Rizzuti, Analysis of the bubbling behaviour of 2d gas solid fluidized beds: part I. Digital image analysis technique, Chemical Engineering Journal 140 (2008) 398–413.
[20] T.W. Asegehegn, M. Schreiber, H.J. Krautz, Investigation of bubble behavior in fluidized beds with and without immersed horizontal tubes using a digital image analysis technique, Powder Technology 210 (2011) 248–260.
[21] E. Truckenbrodt, Fluidmechanik, Springer-Verlag, Berlin, 4, ergänzte aufl. 1999; nachdruck 2008 in veränderter ausstattung. edition, 2008.
[22] L. Böswirth, Technische Strömungslehre: Lehr- und Übungsbuch, Friedr. Vieweg & Sohn Verlag/GWV Fachverlage, Wiesbaden, 2007 Wiesbaden, 7., überarbeitete und erw edition.
[23] R. Clift, W.H. Gauvin, Motion of entrained particles in gas streams, The Canadian Journal of Chemical Engineering 49 (1971) 439–448.
[24] O. Gryczka, S. Heinrich, V. Miteva, N. Deen, J. Kuipers, M. Jacob, L. Mörl, Characterization of the pneumatic behavior of a novel spouted bed apparatus with two adjustable gas inlets, Chemical Engineering Science (2008) 791–814.
[25] J. Richardson, W. Zaki, Sedimentation and fluidization: part 1, Transactions of the Institution of Chemical Engineers 32 (1954) 35–53.

[26] C. Wen, Y. Yu, Mechanics of fluidization, Chemical Engineering Progress Symposium Series 62 (1966) 100–111.
[27] J. Westerweel, Fundamentals of digital particle image velocimetry, Measurement Science and Technology (1997) 1379–1392.
[28] M. Raffel, C.E. Willert, S.T. Wereley, J. Kompenhans, Particle Image Velocimetry: A Practical Guide; with 42 Tables, 2 edition Springer, Berlin, 2007.
[29] J. Link, C. Zeilstra, N.G. Deen, J.A.M. Kuipers, Validation of a discrete particle model in a 2d spout-fluid bed using non-intrusive optical measuring techniques, The Canadian Journal of Chemical Engineering (2004) 30–36.
[30] M.S. van Buijtenen, W.-J. van Dijk, N.G. Deen, J.A.M. Kuipers, T. Leadbeater, D.J. Parker, Numerical and experimental study on multiple-spout fluidised beds, Chemical Engineering Science 66 (2011) 2368–2376.